Journal of the Iranian Chemical Society
https://doi.org/10.1007/s13738-018-1368-1

ORIGINAL PAPER

One-pot three-component process for the synthesis of substituted pyrano[2,3-*c*]pyrazoles catalyzed by nanostructured FSM-16-SO_3H

Somayeh Hashemi-Uderji[1] · Mohammad Abdollahi-Alibeik[1]

Received: 7 July 2017 / Accepted: 15 April 2018

Abstract
A three-component process for the one-pot synthesis of 6-amino-4-aryl-5-cyano-3-methyl-1-phenyl-1,4-dihydropyrano[2,3-*c*]pyrazoles by the reaction of aldehydes, 3-methyl-1-phenyl-1*H*-pyrazol-5(4*H*)-one, and malononitrile in the presence of FSM-16-SO_3H as an efficient mesoporous catalyst. The FSM-16-SO_3H was prepared and characterized by SEM, XRD, BET, and FT-IR techniques. The advantages of the presented method are high yields, short reaction times, easy purification of products, easy work-up, and reusability of the catalyst.

Keywords FSM-16 · FSM-16-SO_3H · Mesoporous silica · Nanocatalyst · Pyranopyrazoles · Multi-component

Introduction

A multi-component reaction (MCR) or a "Multi-component Assembly Process" (MCAP) is a convergent reaction, in which three or more materials incorporate together to form a single production [1], where basically, all of the atoms participate to the newly formed product. MCRs have important role in the synthesis of chemical compounds.

The synthesis of fused pyran derivatives is partial of multi-component reaction (MCR). Nowadays, substituted pyrano[2,3-*c*]pyrazoles are considered as remarkable compounds because of pharmaceutical attributes [2–4]. They represent a perfect range of biological activities including anti-inflammatory [5], antimicrobial [6], anticancer [2, 7], and inhibitors of human Chk1 kinase [8].

The first synthetic procedure of this compounds has been reported by Junek et al. via the reaction of tetracyanoethylene and 3-methyl-1-phenylpyrazolin-5-one [9]. Another method for the synthesis of 6-amino-5-cyano-4-aryl-4*H*-pyrazolo[3,4-b]pyrans includes the reaction of arylidienemalononitrile with 3-methylpyrazoline-5-ones or by the condensation of malononitrile and 4-arylidienepyrazoline-5-one [10]. General method for the synthesis of pyranopyrazole derivatives using three-component reaction is the reaction between pyrazolone, an aldehyde and malononitrile in the presence of various catalyst such as *p*-dodecylbenzene sulfonic acid (DBSA) [11], triethylbenzylammonium chloride (TEBA) [12], hexadecyltrimethylammonium bromide (HTMAB) [13], BF_3/MNPs [14], $H_{14}[NaP_5W_{30}O_{110}]$ [15], MgO [16], and KF·$2H_2O$ [17].

Heterogeneous catalysis has emerged considerable attention in organic transformations, especially in organic industry. The greatest advantage of this type of catalyst compound is the ease of separation. The mesoporous inorganic materials, especially mesoporous silica compounds, are the most important material for the preparation of heterogeneous catalyst.

Mesoporous silica with highly ordered pores and high surface area, such as MCM-41 and FSM-16, has attracted considerable interests in the field of electrochemistry, adsorption science and catalysis chemistry [18–30].

The first reported method for the synthesis of folded sheet mesoporous material (FSM-16) includes intercalation of a layered, kanemite-type sodium silicate with cetyltrimethylammonium (CTMA) ions [18]. FSM-16 is formed via a folded sheet mechanism in which the condensation of the reactive silanol groups available on the vicinal silicate layers in CTMA kanemite complex terminate to the formation of a hexagonal array of channels with the same pore size [19].

Acidity of this mesoporous catalyst is not severe. For this reason, many functional groups have been binded on its surface, to improve the catalytic activity of FSM-16 [31–33].

✉ Mohammad Abdollahi-Alibeik
abdollahi@yazd.ac.ir; moabdollahi@gmail.com

[1] Department of Chemistry, Yazd University, Yazd 89158-13149, Iran

Published online: 27 April 2018

In this research, we report the preparation and characterization of FSM-16-SO_3H as a novel heterogeneous acid catalyst by functionalization of silanol groups on the surface of FSM-16 with –SO_3H groups (Scheme 1).

The catalytic activity of FSM-16-SO_3H was also studied in the reaction of various types of aldehydes, 3-methyl-1-phenyl-1*H*-pyrazol-5(4*H*)-one and malononitrile for the synthesis of pyrano[2,3-*c*]pyrazoles (Scheme 2).

Experimental

Materials and methods

All chemicals were commercial and were used as received. The reactions were monitored by TLC. The yields of products refer to isolated compounds. Melting points were obtained by a Buchi B-540 apparatus and are uncorrected. ^{1}H NMR and ^{13}C NMR spectra of pyranopyrazoles were recorded in DMSO-d_6 on a Bruker DRX-400 AVANCE spectrometer (400 MHz for ^{1}H and 100 MHz for ^{13}C). Infrared spectra of the reaction products and catalysts were recorded on a Bruker FT-IR Equinax-55 in KBr disks. The XRD patterns were recorded on a Bruker D8 ADVANCE

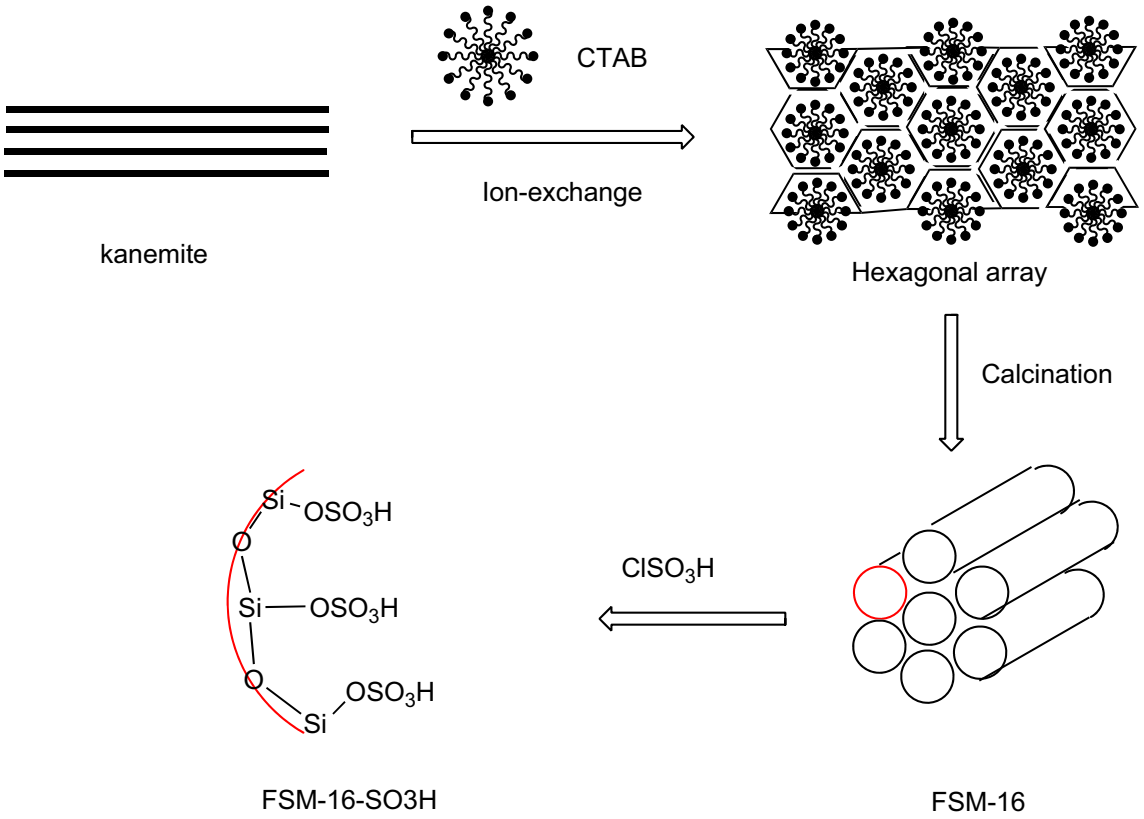

Scheme 1 Schematic representation for the preparation of FSM-16-SO_3H

Scheme 2 Synthesis of pyrano[2,3-*c*]pyrazoles in the presence of FSM-16-SO_3H

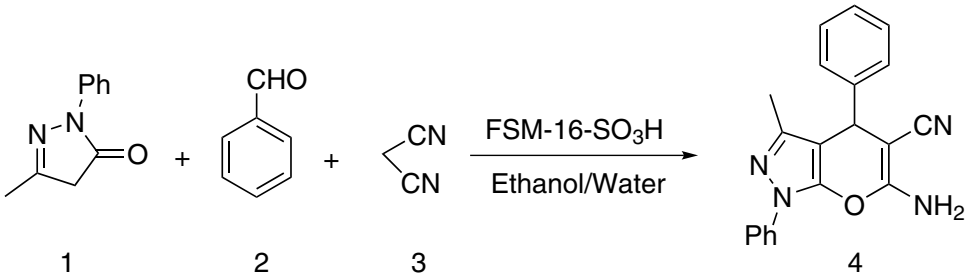

X-ray diffractometer using Ni-filtered Cu Kα radiation. The morphology was studied using a KYKY-EM3200 scanning electron microscope. The BET surface area was measured using a micromeritics model ASAP2020 from the nitrogen adsorption–desorption isotherms at 77 K. All samples were degassed at 120 °C under flowing nitrogen for 2 h. The specific surface area (S_{BET}) was calculated from the adsorption data using the BET equation, and the pore volume (V_{pore}) was estimated from the volume of adsorbed N_2 at relative pressure ($p/p°$) of 0.99. The pore size distribution was calculated by the Barret–Joyner–Halenda (BJH) method.

Preparation of FSM-16 nanoparticles

A typical procedure for the preparation of kanemite was as follows: to a solution of NaOH (3 g) dissolved in deionized water (30 mL), tetraethyl orthosilicate (16.6 mL) was added dropwise and then the mixture was stirred for another 12 h at room temperature. The solution was transferred into an oven and heated at 355 K for 4 h. The resultant product was calcined at 923 K for 5 h to obtain δ-$Na_2Si_2O_5$ (kanemite). The kanemite was deliquescent and immediately used for further treatment. Kanemite (5 g) was dispersed in deionized water (50 mL) and then stirred for 3 h at 300 K. Then, the suspension was filtered out to obtain wet kanemite paste. All of the kanemite pastes were dispersed in an aqueous solution (40 mL) of cetyltrimethylammonium bromide (CTAB) (0.125 mol L^{-1}) and then stirred at 343 K for 3 h. The pH value of the suspension was 11.5–12.5 at this stage. Afterwards, the pH value was adjusted carefully to 8.5 by adding 2 mol L^{-1} hydrochloric acid with stirring. The suspension was kept under stirring at 343 K for 3 h with keeping the pH value at 8–9. After cooling to r.t., the solid was separated by a centrifuge and washed with distilled water (20 mL) and dried in oven at 393 K for 2 h to yield mesoporous silicate, FSM-16, with retaining the template. The product was calcined at 823 K to burn off the surfactant to obtain the final FSM-16.

Preparation of FSM-16-SO_3H nanoparticles

FSM-16 (0.278 g) was added to dry CH_2Cl_2 (3 mL) in a 5 mL round bottom flask equipped with a gas outlet tube and a dropping funnel containing a solution of chlorosulfonic acid (0.6 mL) in dry CH_2Cl_2 (4.5 mL). The chlorosulfonic acid solution was added dropwise to the obtained suspension over a period of 30 min at room temperature. After completion of the reaction, the sediment was separated by a centrifuge and then washed with deionized water (2×3 mL). The obtained solid was dried in an oven at 120 °C for 2 h to obtain FSM-16-SO_3H.

General procedure for the synthesis of pyrano[2,3-*c*] pyrazoles

A mixture of aryl aldehyde (1 mmol), malononitrile (1.1 mmol), 3-methyl-1-phenyl-2-pyrazoline-5-one (1 mmol), and FSM-16-SO_3H (40 mg) was stirred in a mixture of water and ethanol (2 mL, 2:8) at reflux condition. After completion of the reaction (monitored by TLC, eluent; *n*-hexane:ethyl acetate, 7:3), the catalyst was separated by a centrifuge and then washed with ethanol (2×3 mL). After evaporation of solvent, the crude products were crystallized from ethanol to give pure products (4a–o).

Physical and spectroscopic data for selected compounds

6-Amino-3-methyl-1,4-diphenyl-1,4-dihydropyrano[2,3-c]-pyrazole-5-carbonitrile (4a) Yellow solid, mp 178–179 °C (Lit. [14] 172–174 °C). ^{1}H NMR (400 MHz, DMSO-d_6): δ (ppm) = 7.79 (d, J = 8.0 Hz, 2H), 7.50 (t, J = 8.0 Hz, 2H), 7.33–7.38(m, 3H), 7.25–7.29 (m, 3H), 7.23 (s, NH_2), 4.69 (s, 1H), 1.79 (s, 3H); ^{13}C NMR (100 MHz, DMSO-d_6): δ (ppm) = 181.0, 159.4, 145.2, 143.6, 137.5, 129.3, 128.5, 127.8, 127.0, 126.1, 119.9, 109.5, 98.6, 58.1, 36.7, 12.5. FT-IR (KBr disk): 733, 1027, 1065, 1125, 1264, 1385, 1444, 1515, 1592, 2198, 3324, 3471 cm^{-1}.

6-Amino-3-methyl-4-(4-chlorophenyl)-1-phenyl-1,4-dihydropyrano[2,3-c]pyrazole-5-carbonitrile (4b) White solid, mp 180–182 °C (Lit. [14] 178–180 °C). ^{1}H NMR (400 MHz, DMSO-d_6): δ (ppm) = 7.79 (d, J = 8.0 Hz, 2H), 7.50 (t, J = 8.0 Hz, 2H), 7.42 (d, J = 8.0 Hz, 2H), 7.30–7.35 (m, 3H), 7.27 (s, NH_2), 4.74 (s,1H), 1.80 (s, 3H); ^{13}C NMR (100 MHz, DMSO-d_6): δ (ppm) = 188.0, 159.3, 145.2, 143.6, 137.5, 129.3, 128.5, 127.8, 127.7, 127.0, 126.1, 119.9, 98.6, 58.1, 36.7, 12.5. FT-IR (KBr disk): 3448, 3323, 2198, 1660, 1519, 1490, 1392, 1128, 756 cm^{-1}.

6-Amino-3-methyl-4-(3-nitrophenyl)-1-phenyl-1,4-dihydropyrano[2,3-c]pyrazole-5-carbonitrile (4i) White solid, mp 187–189 °C (Lit. [14] 190–191 °C). ^{1}H NMR (400 MHz, DMSO-d_6): δ (ppm) = 8.16–8.17 (m, 2H), 7.79 (m, 3H), 7.68 (t,1H, J = 8.0 Hz), 7.51 (t, 2H, J = 8.0 Hz), 7.38 (s, NH_2), 7.34 (t, 1H, J = 8.0 Hz), 4.98 (s, 1H), 1.81 (s, 3H); ^{13}C NMR (100 MHz, DMSO-d_6): δ (ppm) = 159.7, 147.9, 145.9, 145.1, 144.0, 137.4, 134.7, 130.3, 129.3, 126.3, 122.2, 120.1, 119.7, 97.6, 57.0, 36.1, 12.6. FT-IR (KBr disk): 3437, 3298, 2194, 1651, 1595, 1517, 1400, 1352,1263, 1122, 1070, 756, 694 cm^{-1}.

6-Amino-3-methyl-4-(4-nitrophenyl)-1-phenyl-1,4-dihydropyrano[2,3-c]pyrazole-5-carbonitrile (4o) White solid, mp 195–198 °C (Lit. [14] 192–194 °C). ^{1}H NMR (400 MHz, DMSO-d_6): δ (ppm) = 8.24 (d, J = 8.8 Hz, 2H), 7.80 (d, J = 8.4 Hz, 2H), 7.59 (d, J = 8.8 Hz, 2H), 7.51 (t, J = 7.6 Hz, 2H), 7.40 (s, NH_2), 7.34 (t, J = 6.4, 1H), 4.94

(s, 1H), 1.80 (s, 3H); ^{13}C NMR (100 MHz, DMSO-d_6): δ (ppm) = 181.4, 159.6, 151.2, 146.6, 145.1, 137.4, 129.3, 129.2, 126.3, 123.9, 120.1, 97.6, 66.6, 36.3,12.5. FT-IR (KBr disk): 3338, 3213, 2191, 1666, 1595, 1517, 1402, 1350, 1132, 821 cm^{-1}.

Results and discussions

The catalyst characterization

The FSM-16 and FSM-16-SO_3H were characterized by FT-IR, SEM, BET, and XRD techniques.

The SEM micrographs of FSM-16 and FSM-16-SO_3H are shown in Fig. 1a, b, respectively. SEM micrographs show spherical nanoparticles with sizes of about 100 nm. Both materials have similar texture and there is no significant difference.

Mesostructure of the FSM-16-SO_3H sample was studied by TEM, as shown in Fig. 2. Porosity of the sample is clear and disordered mesoporous system is due to the insertion of sulfonic acid groups on the inner surface of the FSM-16 framework that also confirms by XRD data.

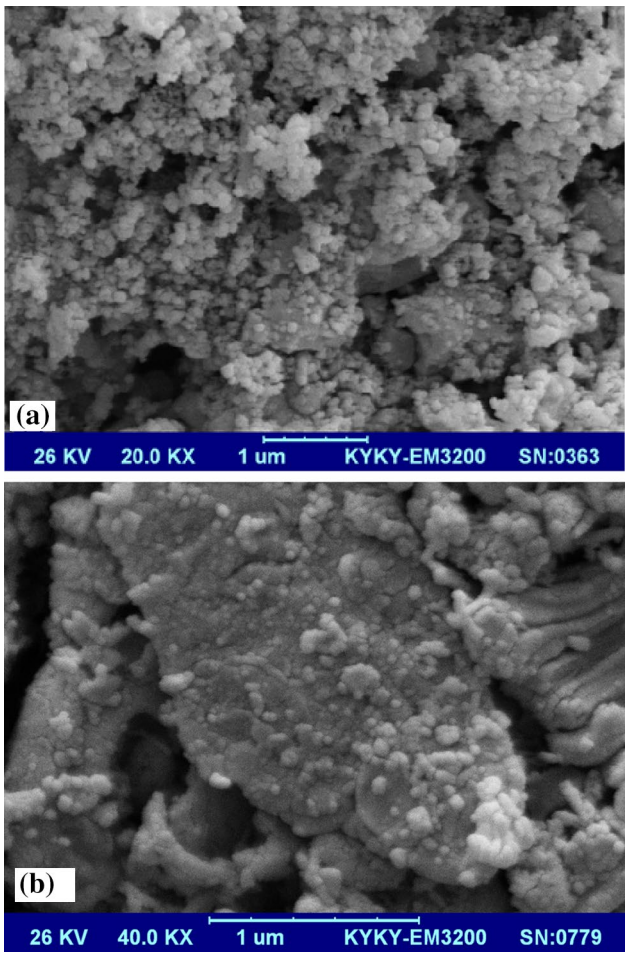

Fig. 1 SEM images of **a** FSM-16 and **b** FSM-16-SO_3H

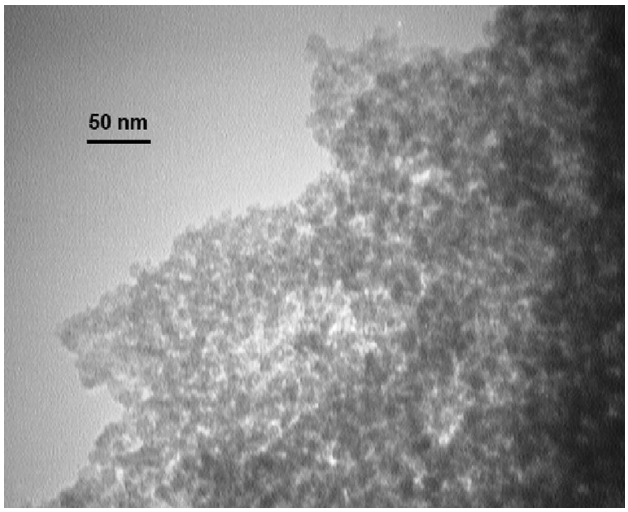

Fig. 2 TEM image of FSM-16-SO_3H

The FT-IR spectra of FSM-16 and FSM-16-SO_3H are shown in Fig. 3. The spectrum of FSM-16 (Fig. 3a) shows characteristic peaks at 1216, 1090, and 804 cm^{-1} due to symmetric and asymmetric stretching vibrations of Si–O–Si and the peak of 966 cm^{-1} due to Si–OH groups. The peak at 463 cm^{-1} is assigned to the bending vibration of Si–O–Si. For FSM-16-SO_3H (Fig. 3b), the FT-IR bands of the O=S=O asymmetric and symmetric stretching modes

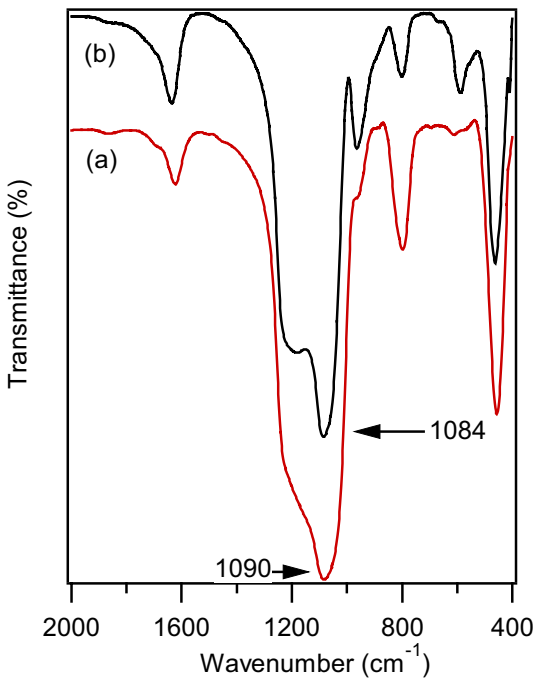

Fig. 3 FT-IR spectra of **a** FSM-16, **b** FSM-16-SO_3H

lies in 1120–1230 and 1010–1080 cm^{-1}, respectively, and that of the S–O stretching mode lies in 600 cm^{-1}. FT-IR spectrum of FSM-16-SO_3H shows the overlap of asymmetric and symmetric stretching bands of SO_2 with Si–O–Si stretching bands in the region of 1000–1250 cm^{-1}, that resulting in increase of intensity of this peak.

The low angle XRD patterns of FSM-16 and FSM-16-SO_3H are shown in Fig. 4. The characteristic peaks of FSM-16 (Fig. 4a) have appeared at $2\theta = 2.38°$, 4.11° and 4.73° in accordance with the literature [34]. As shown in Fig. 4b, after surface modification with SO_3H groups, the intensity of the main peak ($2\theta = 2.38°$) was decreased and shifted to the higher angle ($2\theta = 2.76°$). Increasing in width of the main peak of the FSM-16-SO_3H is due to the decrease in the long-range order of the hexagonal mesostructure of FSM-16 after the incorporation of –SO_3H groups into the channels of FSM-16. The shift of main peak of FSM-16-SO_3H to higher angle is due to decrease in the pore diameter because of the insertion of sulfonic acid groups on the inner surface of mesopores.

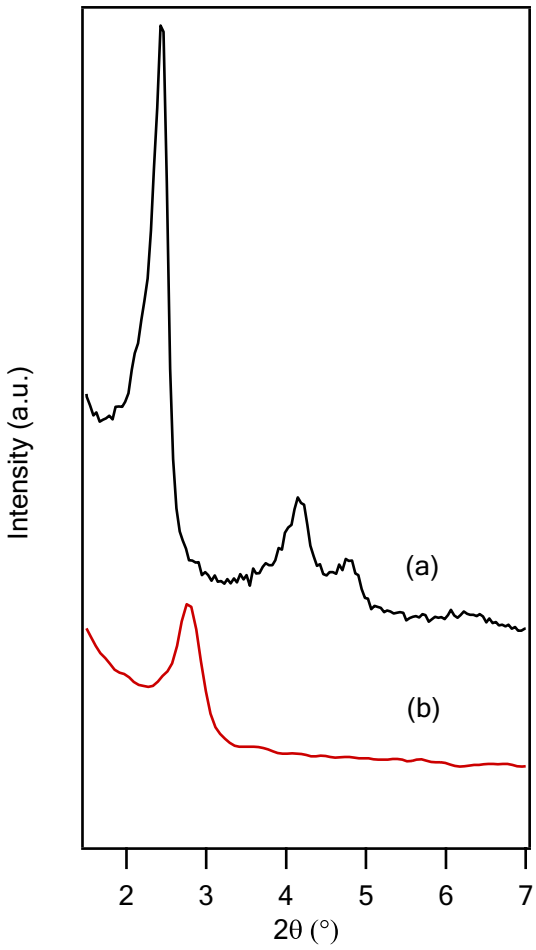

Fig. 4 Low angle XRD patterns of **a** FSM-16, **b** FSM-16-SO_3H

The distribution of both Brønsted and Lewis acid sites of FSM-16-SO_3H was detected using FT-IR spectroscopy by means of pyridine absorption. Figure 5 shows the pyridine adsorbed spectra of FSM-16-SO_3H heated at various temperatures. The spectrum of pyridine adsorbed FSM-16 shows only peaks of pyridine bonded Lewis acid sites at 1446 and 1598 cm^{-1} (Fig. 5b). The spectrum of pyridine adsorbed FSM-16-SO_3H before heat treatment (Fig. 5c) shows the contribution of the pyridine adducts in the region of 1400–1650 cm^{-1}. The peak at 1487 cm^{-1} is attributed to the combination of pyridine bonded to Lewis and Brønsted acid sites. The peaks appearing at 1530 cm^{-1} is assigned to Brønsted acid sites (pyridinum ion). The peak at 1603 cm^{-1} is attributed to the pyridine bonded Lewis acid sites of the

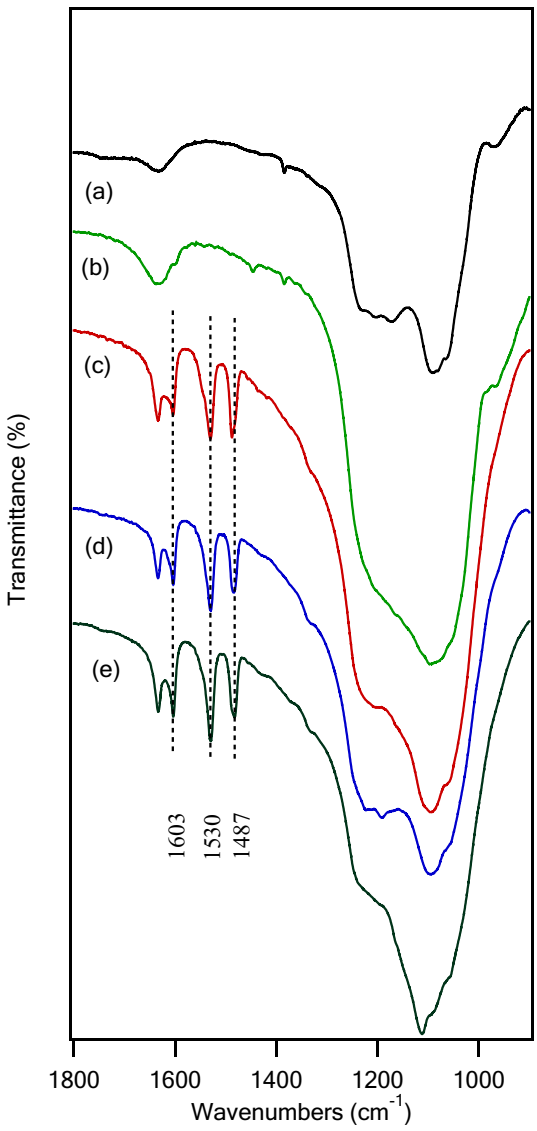

Fig. 5 FT-IR spectra of **a** FSM-16-SO_3H, **b** pyridine adsorbed FSM-16 and **c** FSM-16-SO_3H at ambient temperature and pyridine adsorbed FSM-16-SO_3H heated at **d** 100 °C, **e** 200 °C

catalyst. The peak at 1633 cm^{-1} in the spectrum of the catalyst before treatment with pyridine (Fig. 5a) is due to the presence of water during the preparation of the pellet sample. This sharp peak overlapped with another weak peak of Brønsted acid sites at 1642 cm^{-1}. However, these results confirm distribution of both Brønsted and Lewis acid sites on the surface of the catalyst. As shown in Fig. 5b–e, with increasing in temperature, characteristic peaks of Lewis acid sites at 1603 cm^{-1} and peaks of Brønsted acid sites at 1530 cm^{-1} are still remained. These results confirm that $–SO_3H$ functionalization has strengthened both Brønsted and Lewis acid sites on the catalyst.

The strength and number of acid sites of the catalysts were determined by potentiometric titration of samples with 0.02 N solution of *n*-butylamine in acetonitrile. According to this method, the initial electrode potential (E_i) indicates the strength of acid sites and meq of the consumed base indicates number of acid sites [23]. As shown in Fig. 6, the very low initial potential of FSM-16 shows that acid strength of these samples is very low. With placing of $–SO_3H$ groups on the surface of FSM-16, FSM-16-SO_3H displays higher strength than the FSM-16. Owing to more meq of the used base per gram of the FSM-16-SO_3H, this sample has also higher number of acidic sites than FSM-16.

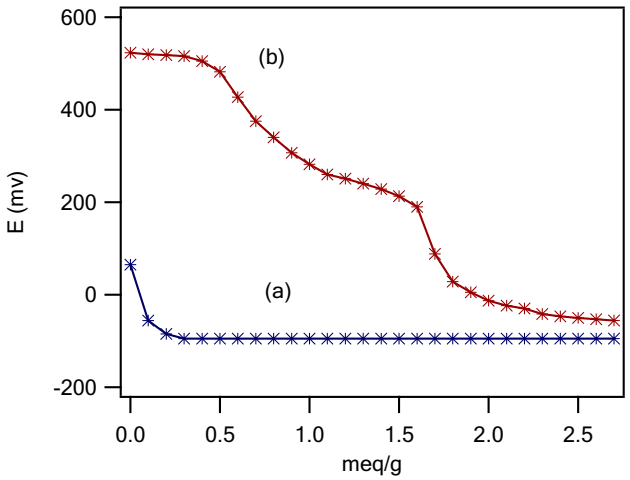

Fig. 6 Potentiometric titration of **a** FSM-16, **b** FSM-16-SO_3H

To investigate the number of $–SO_3H$ acidic sites supported on the FSM-16, the elemental composition of the FSM-16-SO_3H using EDX analysis was determined and results are shown in Fig. 7 and Table 1. Based on this result, amount of sulfur in the FSM-16-SO_3H is 7.08 wt%, and thus, the number of $–SO_3H$ on the catalyst is 0.87 mmol per gram of FSM-16-SO_3H.

Figure 8 shows the N_2 adsorption–desorption isotherms of the FSM-16 and FSM-16-SO_3H catalysts. In the isotherms of FSM-16, a mesoporous inflection was observed at the medium $p/p°$ partial pressure region ($p/p° = 0.1–0.3$), due to the capillary condensation of N_2 in the mesopores. A sharper hysteresis was observed at higher $p/p°$ ($p/p° > 0.8$) for both catalysts. The hysteresis in this region is because of the condensation of N_2 within the voids formed by nanoparticles. In the isotherms of FSM-16-SO_3H, the curvature of the mesoporous structure in the area of $p/p°$=0.2–0.4 is decreased because of occupation of the hexagonal cavities by $–SO_3H$ groups.

Table 1 Elemental composition of FSM-16-SO_3H

Element	O	Si	S
wt%	61.31	31.60	7.08

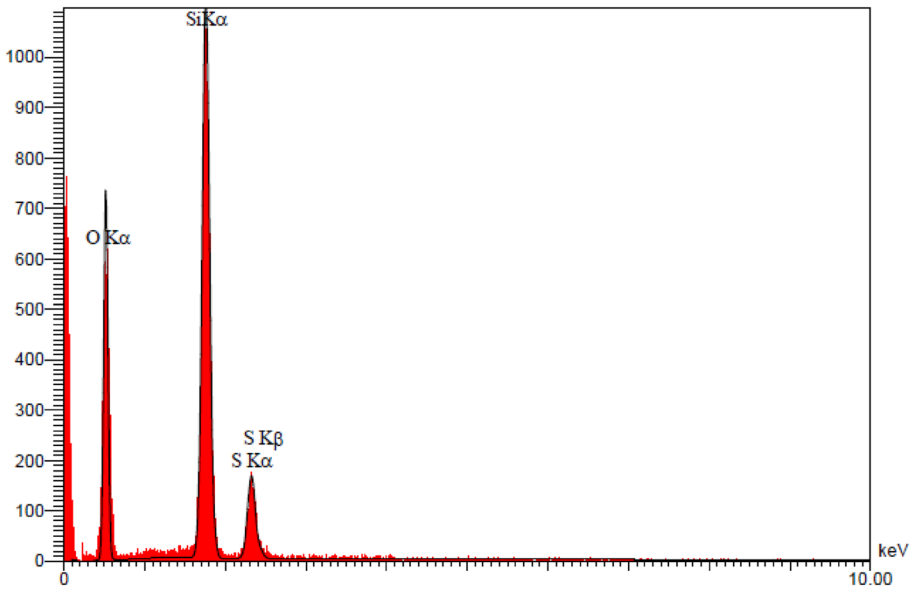

Fig. 7 Energy-dispersive X-ray spectrum of FSM-16-SO_3H

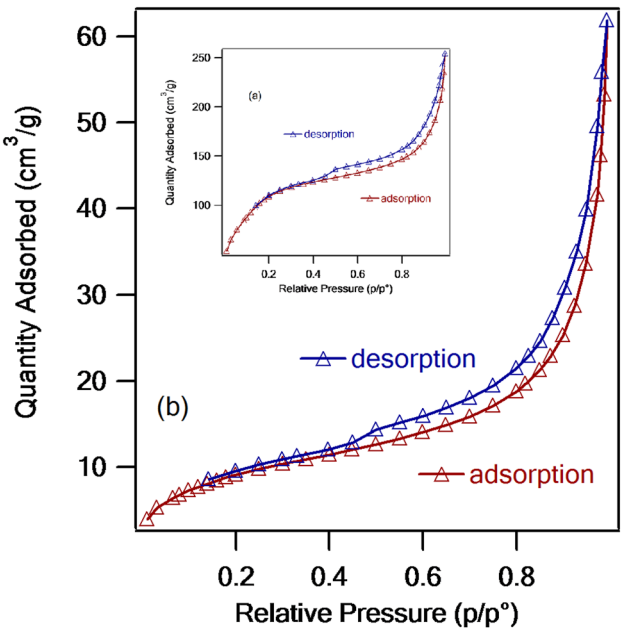

Fig. 8 N_2 adsorption–desorption isotherms of **a** FSM-16, **b** FSM-16-SO_3H

Catalytic activity of FSM-16-SO_3H

The catalytic activity of FSM-16-SO_3H was investigated in the multi-component reaction of benzaldehyde (1 mmol), malononitrile (1.1 mmol) and 3-methyl-1-phenyl-1*H*-pyrazol-5(4*H*)-one (1 mmol) as model reaction for the synthesis of pyrano[2,3-*c*]pyrazole. The reaction was optimized for various parameters such as catalyst amount, temperature, and solvent.

The effect of solvent and temperature was investigated by performing the model reaction in the presence of 40 mg catalyst in various solvents and temperatures (Table 2, entries 1–7). Among them, the mixture of water and ethanol was found to be the best solvent under reflux condition in terms of the reaction time and yield of product (Table 2, entry 7). The lower yield and longer reaction time was achieved by performing the model reaction in the presence of ethanol as the solvent under reflux conditions and at room temperature (Table 2, entry 5, 6).

To optimize the required catalyst amount, the model reaction was also performed in the presence of various amounts of the catalyst and according to the obtained results (Table 2, entries 8–14) 40 mg of the catalyst was chosen as the best catalyst amount. Clearly, the FSM-16 support strongly affected the efficiency of the heterogeneous catalyst. To show this, the model reaction in the presence of 40 mg FSM-16 was performed under the same reaction conditions and lower yield of the product was obtained after 105 min (Table 2, entry 9).

Table 2 Optimization of the reaction conditions for the synthesis of pyrano[2,3-*c*]pyrazoles catalyzed by FSM-16-SO_3H

Entry	Catalyst	Catalyst amount (mg)	Solvent	Time (min)	Yield (%)[a]
1	FSM-16-SO_3H	40	$CHCl_3$	240	75
2	FSM-16-SO_3H	40	CH_2Cl_2	310	78
3	FSM-16-SO_3H	40	MeOH	50	83
4	FSM-16-SO_3H	40	CH_3CN	60	80
5	FSM-16-SO_3H	40	EtOH[b]	270	80
6	FSM-16-SO_3H	40	EtOH	50	85
7	FSM-16-SO_3H	40	EtOH/water	40	88
8	–	0	EtOH/water	240	60
9	FSM-16	40	EtOH/water	105	75
10	FSM-16-SO_3H	10	EtOH/water	70	60
11	FSM-16-SO_3H	20	EtOH/water	65	71
12	FSM-16-SO_3H	30	EtOH/water	55	79
13	FSM-16-SO_3H	50	EtOH/water	50	79
14	FSM-16-SO_3H	60	EtOH/water	55	80

Reactions were carried out under reflux condition with benzaldehyde (1 mmol), malononitrile (1.1 mmol) and 3-methyl-1-phenyl-1*H*-pyrazol-5(4*H*)-one (1 mmol)

[a]Isolated yield

[b]Reaction was carried out under r.t.

Afterwards, the optimized reaction conditions were performed for the synthesis of 1,4-dihydropyrano[2,3-*c*] pyrazoles using various aromatic aldehydes and results are summarized in Table 3. It was found that this method is rather general for both, electron rich and electron poor aryl aldehydes and the corresponding products were obtained in good to excellent yields.

To investigate the reusability of FSM-16-SO_3H, it was separated from the reaction mixture and washed with ethanol. The catalyst was dried in oven at 120 °C for 2 h. The recycled catalyst was reused in the model reaction. The catalyst was found to be reusable for at least three cycles without considerable loss of activity (Table 4).

A plausible mechanism for the synthesis of pyrano[2,3-*c*] pyrazoles in the presence of FSM-16-SO_3H is illustrated in Scheme 3.

Table 3 Synthesis of pyrano[2,3-*c*]pyrazoles catalyzed by FSM-16-SO_3H

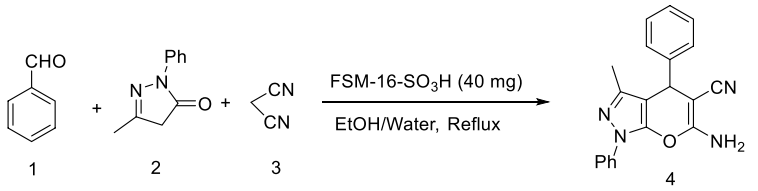

Entry	1	4	Time (min)	Yield (%)[a]
a		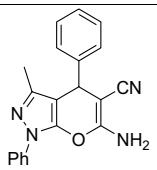	40	88
b	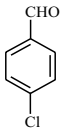	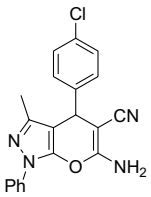	30	82
c	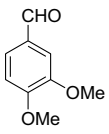	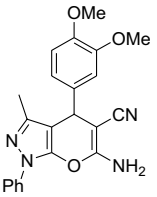	60	79
d	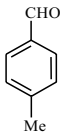	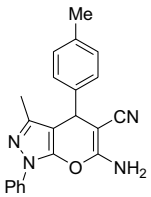	30	85
e	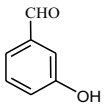	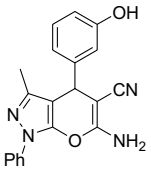	27	78
f	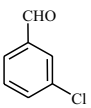	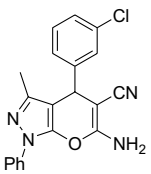	35	81
g	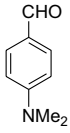	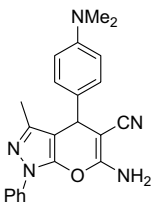	27	85

Table 3 (continued)

Entry	1	4	Time (min)	Yield (%)[a]
h	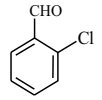	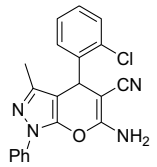	65	80
I	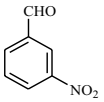	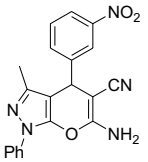	25	80
j	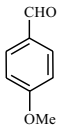	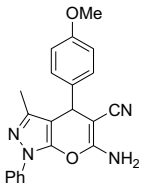	95	76
k	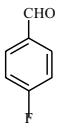	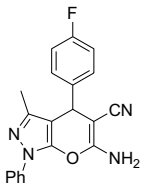	20	83
l		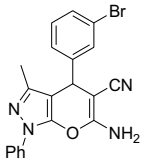	35	82
m	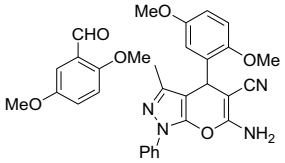		10	70
n	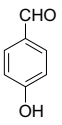	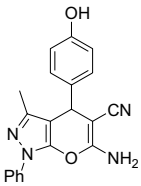	50	78
o	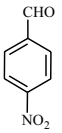	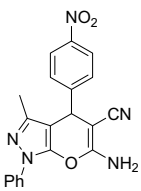	30	81

Reaction conditions: aldehyde (1 mmol), malononitrile (1.1 mmol), 3-methyl-1-phenyl-1*H*-pyrazol-5(4*H*)-one (1 mmol), FSM-16-SO_3H (40 mg), ethanol:water; 8:2 (2 mL), 100 °C

[a]Isolated yield

Table 4 Recycling of FSM-16-SO_3H nanoparticles

Run	Yield (%)[a]	Time
1	88	40
2	88	50
3	85	65

Reaction conditions: aldehyde (1 mmol), malononitrile (1.1 mmol), 3-methyl-1-phenyl-1*H*-pyrazol-5(4*H*)-one (1 mmol), FSM-16-SO_3H (40 mg), ethanol:water; 8:2 (2 mL), 100 °C

[a]Isolated yield

Table 5 shows the comparison between the activity of the FSM-16-SO_3H and other reported catalysts for the pyrano[2,3-*c*]pyrazoles synthesis through reaction of benzaldehyde, malononitrile and 3-methyl-1-phenyl-1*H*-pyrazol-5(4*H*)-one. Results show that FSM-16-SO_3H is comparable with other catalytic systems in term of yield and/or reaction time. In addition to this, easy work-up and using a reusable catalyst are other benefits of this method.

Conclusion

In summary, we have developed a novel, mild and efficient strategy for the synthesis of pyrano[2,3-*c*]pyrazoles from aryl aldehydes, malononitrile and 3-methyl-1-phenyl-1*H*-pyrazol-5(4*H*)-one using FSM-16-SO_3H as solid acid catalyst. The catalyst was prepared and characterized by SEM, BET, XRD, pyridine absorption, potentiometric titration and FT-IR techniques. Results show that FSM-16-SO_3H is an efficient catalyst with easy recoverability and reusability without significant decrease in catalytic activity. The methodology is simple, rapid, and relatively inexpensive affording good to excellent yields with operational simplicity.

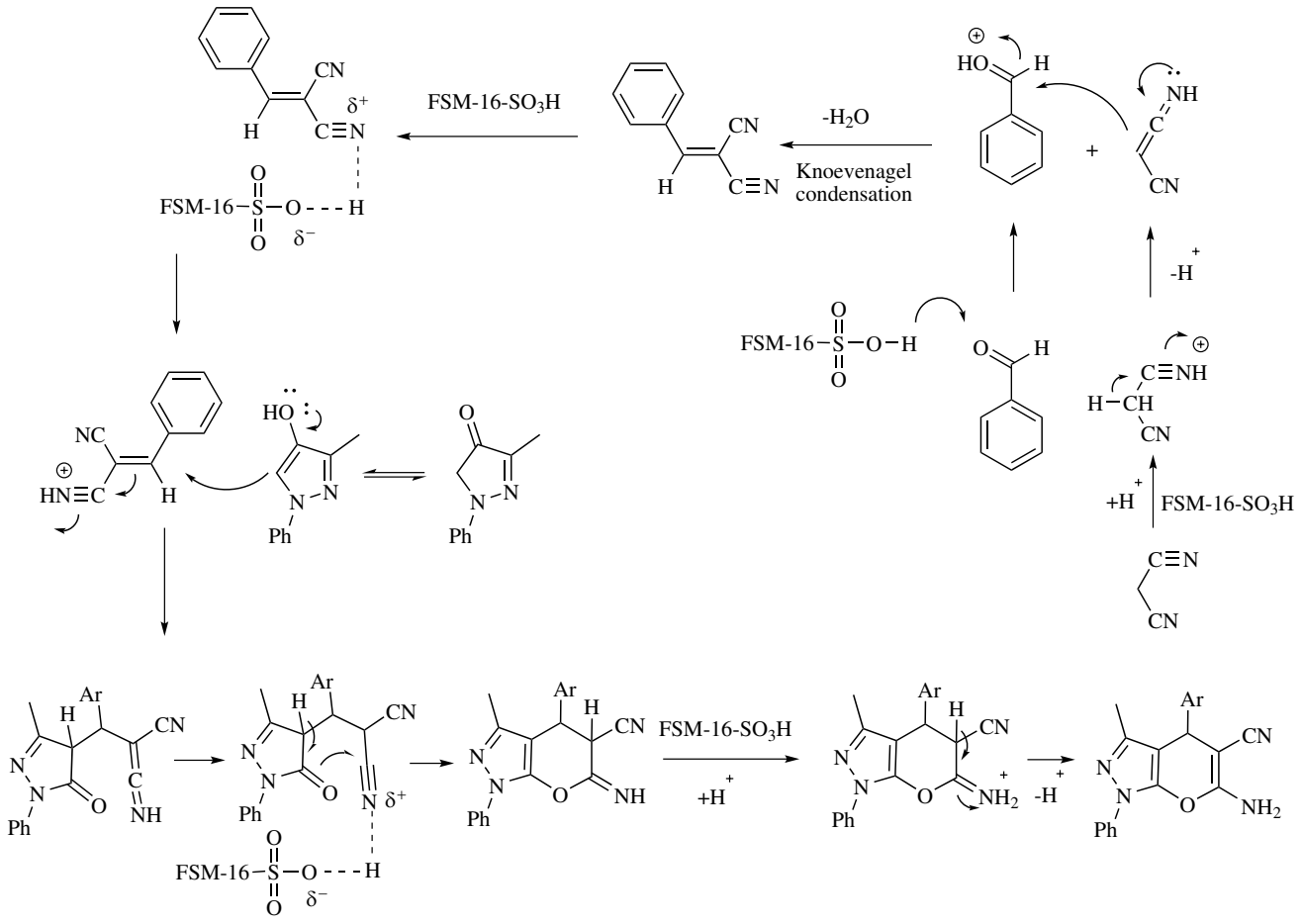

Scheme 3 Plausible mechanism for the synthesis of pyrano[2,3-*c*]pyrazoles in the presence of FSM-16-SO_3H

Table 5 Comparative study of the activity of FSM-16-SO_3H with other catalysts

Entry	Catalyst	Solvent	Temp (°C)	Time (min)	Yield[a] (%)	References
1	FSM-16-SO_3H	Ethanol/water	Reflux	40	88	This work
2	DBSA (10 mol%)	Water	60	180	88	[11]
3	$H_{14}[NaP_5W_{30}O_{110}]$	Ethanol	Reflux	60	84	[15]
4	HTMAB	Water	85–90	180	89	[13]
5	TEBA	Water	90	360	99	[12]
6	[Sipim]HSO_4	Solvent free	110	90	92	[35]
7	$NH_4H_2PO_4/Al_2O_3$	Ethanol	Reflux	15	84	[36]
8	Sulfamic acid	Ethanol	Reflux	600	82	[37]

[a]Isolated yield

Acknowledgements We are thankful to the Yazd University Research Council for partial support of this work.

References

1. R.W. Armstrong, A.P. Combs, P.A. Tempest, S.D. Brown, T.A. Keating, Acc. Chem. Res. **29**, 123 (1996)
2. J.-L. Wang, D. Liu, Z.-J. Zhang, S. Shan, X. Han, S.M. Srinivasula, C.M. Croce, E.S. Alnemri, Z. Huang, Proc. Natl. Acad. Sci. **97**, 7124, (2000)
3. J. Wang, O. Novaro, X. Bokhimi, T. Lopez, R. Gomez, J. Navarrete, M. Llanos, E. Lopez-Salinas, J. Phys. Chem. B **101**, 7448 (1997)
4. K.L. Kees, J.J. Fitzgerald, K.E. Steiner, J.F. Mattes, B. Mihan, T. Tosi, D. Mondoro, M.L. McCaleb, J. Med. Chem. **39**, 3920 (1996)
5. M.E. Zaki, H.A. Soliman, O.A. Hiekal, A.E. Rashad, Z. Naturforsch, C Biosci. **61**, 1 (2006)
6. P.W. Smith, S.L. Sollis, P.D. Howes, P.C. Cherry, I.D. Starkey, K.N. Cobley, H. Weston, J. Scicinski, A. Merritt, A. Whittington, J. Med. Chem. **41**, 787 (1998)
7. M. Zaki, E. Morsy, F. Abdel-Motti, F. Abdel-Megeid, Heterocycl. Commun. **10**, 97 (2004)
8. N. Foloppe, L.M. Fisher, R. Howes, A. Potter, A.G. Robertson, A.E. Surgenor, Bioorg. Med. Chem. **14**, 4792 (2006)
9. H. Junek, H. Aigner, Chem. Ber. **106**, 914 (1973)
10. H. Wamhoff, E. Kroth, C. Strauch, Synthesis **1993**, 1129 (1993)
11. T.-S. Jin, R.-Q. Zhao, T.-S. Li, Arkivoc **2006**, 176 (2006)
12. D. Shi. J. Mou, Q. Zhuang, L. Niu, N. Wu, X. Wang, Synth. Commun. **34**, 4557 (2004)
13. T.S. Jin, A.Q. Wang, Z.L. Cheng, J.S. Zhang, T.S. Li, Synth. Commun. **35**, 137 (2005)
14. M. Abdollahi-Alibeik. A. Moaddeli, K. Masoomi, RSC Adv. **5**, 74932 (2015)
15. M. Heravi, A. Ghods, F. Derikvand, K. Bakhtiari, F. Bamoharram, J. Iran. Chem. Soc. **7**, 615 (2010)
16. H. Sheibani, M. Babaie, Synth. Commun. **40**, 257 (2009)
17. Z. Ren, W. Cao, W. Tong, Z. Jin, Synth. Commun. **35**, 2509 (2005)
18. T. Yanagisawa, T. Shimizu, K. Kuroda, C. Kato, Bull. Chem. Soc. Jpn. **63**, 988 (1990)
19. S. Inagaki, Y. Fukushima, K. Kuroda, J. Chem. Soc. Chem. Commun. 680 (1993)
20. S. Inagaki, A. Koiwai, N. Suzuki, Y. Fukushima, K. Kuroda, Bull. Chem. Soc. Jpn. **69**, 1449 (1996)
21. C.T. Kresge, M.E. Leonowicz, W.J. Roth, J.C. Vartluti, J.S. Beck, Nature **359**, 710 (1992)
22. J. Beck, J. Vartuli, W. Roth, M. Leonowicz, C. Kresge, K. Schmitt, C. Chu, D. Olson, E. Sheppard, J. Am. Chem. Soc. **114**, 10834 (1992)
23. M. Abdollahi-Alibeik, I. Mohammadpoor-Baltork, Z. Zaghaghi, B.H. Yousefi, Catal. Commun. **9**, 2496 (2008)
24. M. Abdollahi-Alibeik, E. Heidari-Torkabad, C. R. Chim. **15**, 517 (2012)
25. M. Abdollahi-Alibeik, M. Pouriayevali, Catal. Commun. **22**, 13 (2012)
26. M. Abdollahi-Alibeik, F. Nezampour, React. Kinet. Mech. Catal. **108**, 213 (2013)
27. M. Abdollahi-Alibeik, A. Rezaeipoor-Anari, J. Magn. Magn. Mater. **398**, 205 (2016)
28. M. Abdollahi-Alibeik, A. Rezaeipoor-Anari, Catal. Sci. Technol. **4**, 1151 (2014)
29. M. Abdollahi-Alibeik, N. Sadeghi-Vasafi, A. Moaddeli, A. Rezaeipoor-Anari, Res. Chem. Intermed. **42**, 2867 (2016)
30. M. Abdollahi-Alibeik, G. Ahmadi, Res. Chem. Intermed. **41**, 8173 (2015)
31. T. Yamamoto, T. Tanaka, S. Inagaki, T. Funabiki, S. Yoshida, J. Phys. Chem. B **103**, 6450 (1999)
32. O. Jakdetchai, N. Takayama, T. Nakajima, Kinet. Catal. **46**, 56 (2005)
33. K. Shimizu, E. Hayashi, T. Hatamachi, T. Kodama, T. Higuchi, A. Satsuma, Y. Kitayama, J. Catal. **231**, 131 (2005)
34. H. Araki, A. Fukuoka, Y. Sakamoto, S. Inagaki, N. Sugimoto, Y. Fukushima, M. Ichikawa, J. Mol. Catal. A Chem. **199**, 95 (2003)
35. K. Niknam, A. Piran, Green Sustain. Chem. **3**, 1 (2013)
36. B. Maleki, S.S. Ashrafi, RSC Adv. **4**, 42873 (2014)
37. S.V. Shinde, W.N. Jadhav, J.M. Kondre, S.V. Gampawar, N.N. Karade, J. Chem. Res. **2008**, 278 (2008)